

Dense Low-Coordination Phases of Lithium

Chris J. Pickard

*Scottish Universities Physics Alliance, School of Physics and Astronomy, University of St. Andrews,
St Andrews, KY16 9SS, United Kingdom*

R. J. Needs

*Theory of Condensed Matter Group, Cavendish Laboratory, Cambridge CB3 0HE, United Kingdom
(Received 17 September 2008; published 7 April 2009)*

Ab initio density-functional-theory calculations and a structure-searching technique are used to identify candidate high-pressure phases of lithium (Li). We predict threefold coordinated structures to be stable in the pressure range 40–450 GPa and fourfold structures at higher pressures. We describe these low-coordination phases as elemental electrides. All of the stable phases are metallic but the *Cmca*-24 structure, and two distortions of it which are marginally the most stable in the pressure range 86–106 GPa, are nearly semiconducting with densities of electronic states at the Fermi energy of only a few percent of the free-electron value.

DOI: 10.1103/PhysRevLett.102.146401

PACS numbers: 71.15.Nc, 61.66.-f, 62.50.-p

In the close-packed structures adopted by Li at low pressures [1] the $2s$ electrons combine to form a half-filled nearly-free-electron band, consistent with the picture of a simple alkali metal. However, strong deviations from the canonical picture develop at higher pressures. Overlap of the Li $1s$ core electrons on neighboring atoms under strong compression has a profound effect upon the structures, which adopt lower coordination structures [2,3].

The close-packed face-centered-cubic (fcc) phase of Li transforms to a structure of $I\bar{4}3d$ space group symmetry [4] at ~ 40 GPa, via an intermediate phase of $R\bar{3}m$ symmetry [3]. The $R\bar{3}m$ phase has a distorted fcc structure, but the $I\bar{4}3d$ structure departs very substantially from close packing. $I\bar{4}3d$ has three short interatomic distances giving threefold coordination. Calculations show that the valence electronic density of states (e-DOS) dips around the Fermi energy (E_F) [3]. These features are consistent with the picture that reduced coordination numbers at high pressures arise from a Jahn-Teller-like distortion [2]. Calculations of the high-pressure phases also show an accumulation of electronic charge density within the interstitial region as the $2s$ electron density is pushed away from the atomic cores by Coulomb repulsion, Pauli exclusion, and the orthogonality of core and valence orbitals [2,3,5].

Experiments suggest another phase transition at 60–70 GPa, although the new structure has not been determined [6,7]. A number of theoretical studies have sought to identify candidate phases at higher pressures [2,8,9]. A DFT study by Rousseau *et al.* [8] found a structure of *Cmca* symmetry to be more stable than $I\bar{4}3d$ above 88 GPa. This structure is named *Cmca*-24, appending the number of atoms in the conventional unit cell [8]. *Cmca*-24 consists of threefold coordinated atoms [8].

Ma *et al.* [9] studied high-pressure phases of Li using a combination of *ab initio* DFT methods and an evolutionary

search algorithm, finding a new structure of $P4_132$ symmetry which they calculated to be more stable than *Cmca*-24 above 300 GPa. This structure contains sixfold coordinated atoms. On the other hand, recent high-temperature DFT molecular dynamics simulations found fourfold coordinated Li atoms in the pressure range 150–810 GPa [10].

Superconductivity has been observed in Li up to ~ 85 GPa, indicating metallic behavior [6,11,12]. However, calculations have suggested that semimetallic or even semiconducting behavior might occur at high pressures [2]. Increases in the electrical resistance of highly compressed Li have also been observed in shock-wave experiments, lending support to this suggestion [13,14].

The lack of experimental information on the high-pressure phases of Li beyond $I\bar{4}3d$, the possibility of semiconducting behavior at high pressures, and differences between the various theoretical predictions motivates the present study. We have searched for candidate high-pressure phases of Li using a combination of *ab initio* calculations and “random structure searching” which we refer to as “AIRSS”. This approach has been applied successfully to a number of systems [15–18]. An ensemble of structures is chosen by first generating random unit cell translation vectors and renormalizing the resulting cell volumes to lie within some reasonable range. The atoms are then placed at random positions and the cell shapes and atomic positions are relaxed at a fixed pressure to a minimum in the enthalpy.

We performed searches at 50 GPa (with 8, 12, and 16 atoms per cell), 75 GPa (12, 16, 24 atoms), 100 GPa (8, 12, 14, 16, 18, 24 atoms) 200 GPa (8, 12, 16 atoms), 400 GPa (4, 8, 12, 16 atoms), 600 GPa (8, 12, 16 atoms), and searches at 1000 and 2000 GPa with 8-atom cells. We

also performed a search at 100 GPa with 24 atoms whose positions were constrained to conform to the $P2_1$ space group which contains two symmetry operations. We used the CASTEP plane-wave code [19], ultrasoft pseudopotentials [20], and the Perdew-Burke-Ernzerhof (PBE) generalized gradient approximation (GGA) density functional [21]. For the searches we used a plane-wave basis set cutoff of 350 eV and the Brillouin zone integrations were performed using a k -point grid of spacing $2\pi \times 0.05 \text{ \AA}^{-1}$. The most interesting structures were further relaxed at a higher level of accuracy consisting of a basis set cutoff of 420 eV and a k -point grid spacing of $2\pi \times 0.03 \text{ \AA}^{-1}$. Very high quality pseudopotentials in which all three electrons are treated explicitly must be used to obtain accurate results. A set of test calculations were performed using pseudopotentials with progressively smaller core radii and the bare Coulomb potential. We concluded that the errors in the enthalpy differences between phases arising from a pseudopotential of core radius 1.2 a.u. are smaller than 10 meV per atom. This pseudopotential was used to obtain the results reported here.

The enthalpies of the more stable phases, calculated at the higher level of accuracy, are plotted as a function of pressure in Fig. 1, and the details of the structures are reported in the auxiliary material [22]. We find the experimentally observed $I\bar{4}3d$ phase to be stable in a range of pressures up to ~ 86 GPa, at which point it becomes unstable to a quite different structure of $Pbca$ symmetry. The $Pbca$ structure is a distortion of $Cmca$ -24 (which has a 12-atom primitive cell) into a 24-atom primitive cell, as illustrated in Fig. 2. At ~ 98 GPa a distortion of $Cmca$ -24 with $Aba2$ symmetry and a 12-atom primitive cell be-

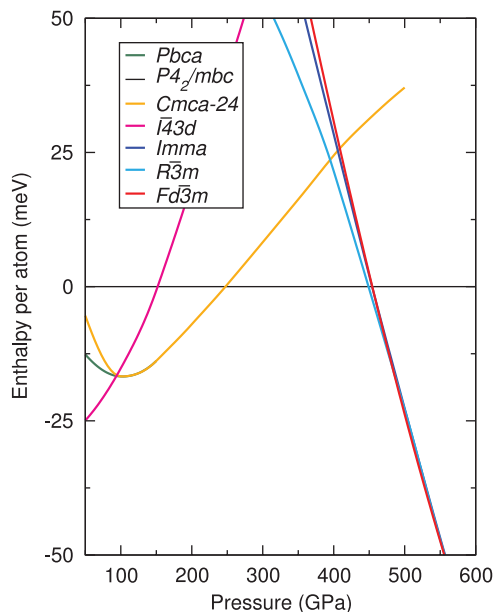


FIG. 1 (color). Variation of the enthalpies of phases of Li with pressure. Differences in enthalpy from the $P4_2/mbc$ phase are plotted.

comes slightly more stable than $Pbca$. (The enthalpy of $Aba2$ is not plotted in Fig. 1 as it is indistinguishable from $Cmca$ -24 on this scale.) The enthalpies of the $Pbca$, $Aba2$, and $Cmca$ -24 phases differ by less than 1 meV per atom at pressures above ~ 85 GPa, which is smaller than our calculational accuracy, but it is clear from Fig. 1 that the $Pbca$ phase is favored at lower pressures and that the structures tend to the higher-symmetry $Cmca$ -24 phase at higher pressures.

All of the low-enthalpy high-pressure phases of Li show a substantial accumulation of electronic charge density within the interstitial regions, as was found in previous theoretical studies [2,3,8]. The valence e-DOS of the $I\bar{4}3d$, $Cmca$ -24, and the much higher enthalpy fcc phase are shown in Fig. 3(a) at 75 GPa. (The occupied e-DOS of the $Pbca$, $Aba2$, and $Cmca$ -24 phases are very similar, see the auxiliary material [22].) The occupied valence bandwidths are 35%–40% smaller than the free-electron bandwidths at the same densities. This narrowing arises because the valence electrons are pushed away from the cores and lie within the interstitial regions. Neighboring interstitial regions are partially cutoff from one another by the cores and the occupied valence bandwidth is reduced [5]. The band narrowing increases the e-DOS in the lower portion of the valence band, and the e-DOS at E_F of the fcc phase is 210% of the free-electron value at the same density. A structure with a large e-DOS at E_F is susceptible to a Jahn-Teller-like distortion and the more stable $I\bar{4}3d$, $Pbca$, $Aba2$, and $Cmca$ -24 phases show very pronounced dips in their e-DOS around E_F . The e-DOS at E_F of $I\bar{4}3d$ is 72% of the free-electron value. The occupied valence bandwidths of $I\bar{4}3d$ and $Cmca$ -24 actually decrease as the pressure is increased from 75 to 100 GPa, while at the same time the e-DOS at E_F decreases. The e-DOS at E_F of $Cmca$ -24 is only 5% of the free-electron value at 75 GPa, and it falls by a factor of 2 by 100 GPa.

The AIRSS method yields structures which are stable against zone-center phonon distortions (including elastic distortions) within the unit cell used for the searches. Additional calculations indicated that the $Pbca$, $Aba2$, and $Cmca$ -24 phases have some soft phonon frequencies at pressures around 100 GPa which are very sensitive to the quality of the Brillouin zone integrations. It is possible that

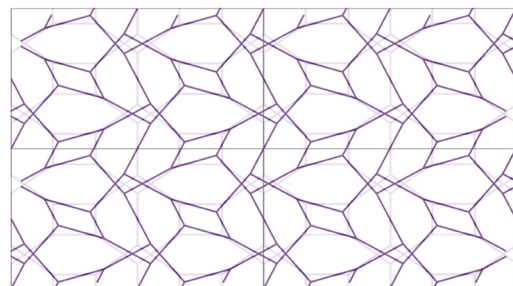


FIG. 2 (color online). Frameworks of the $Pbca$ (dark) and $Cmca$ -24 (light) structures at 75 GPa. The cell vectors of $Pbca$ have been scaled slightly to equal those of $Cmca$ -24.

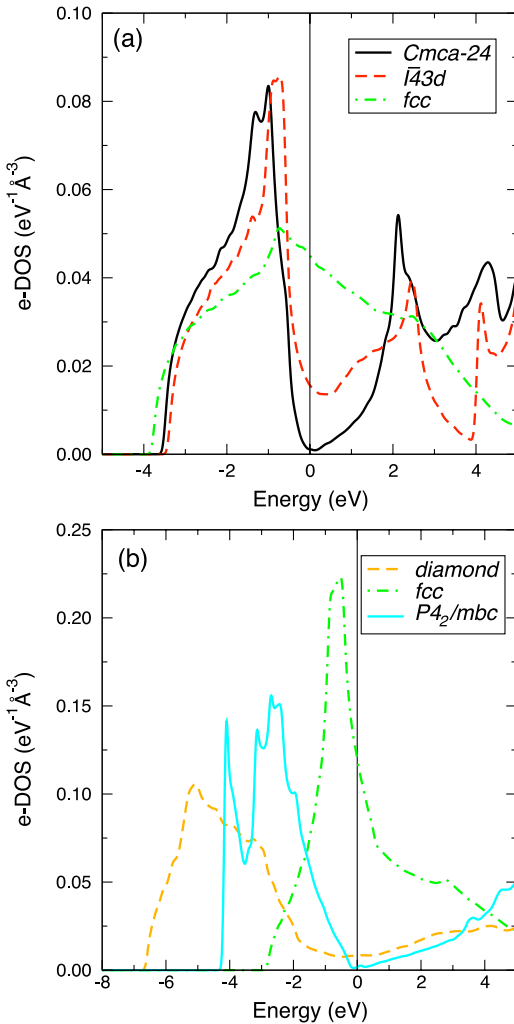


FIG. 3 (color online). Valence electronic densities of states (e-DOS) of selected phases (a) at 75 GPa and (b) at 450 GPa. The zero of energy is placed at E_F .

other structures with similar bonding might exist in this pressure range which are slightly more stable than the ones we have found. The existence of several similar structures which are almost degenerate in enthalpy suggests that disordered structures might be obtained in experiments. The combination of structural disorder and very low e-DOS around E_F could even result in semiconducting behavior.

We find the *Cmca-24* phase to be the most stable above 106 GPa, and Tse *et al.* [23] have shown that this phase has stable phonon modes at high pressures. We have found several new structures at higher pressures. A structure of $P4_2/mbc$ symmetry is shown in Fig. 4 which becomes more stable than *Cmca-24* at 247 GPa. We found the phonons of $P4_2/mbc$ to be stable across the entire Brillouin zone, see the auxiliary material [22]. $P4_2/mbc$ is predicted to be stable up to 449 GPa where it yields to a new structure of $R\bar{3}m$ symmetry, which is in turn replaced by the diamond structure (space group $Fd\bar{3}m$) at 483 GPa. The $R\bar{3}m$, diamond structure, and *Imma* phases are almost

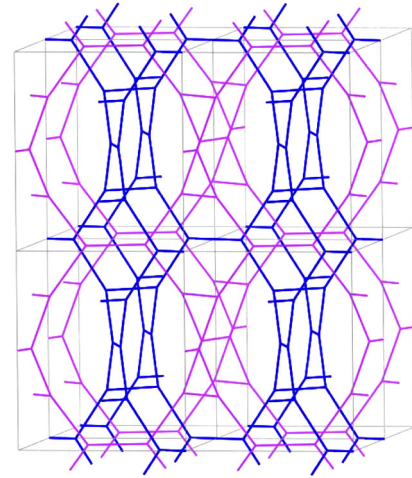


FIG. 4 (color online). Framework of the $P4_2/mbc$ structure at 250 GPa. The different colors indicate the two interpenetrating threefold coordinated networks.

degenerate above ~ 450 GPa and, in fact, the $R\bar{3}m$ and *Imma* structures are small distortions of the diamond structure at these pressures, which explains why they are so nearly degenerate. The diamond structure is calculated to be stable to pressures beyond 1 TPa.

$P4_2/mbc$ is a threefold coordinated structure composed of two separate but inter-penetrating threefold coordinated networks, as illustrated in Fig. 4. The $R\bar{3}m$, diamond, and *Imma* structures have fourfold coordination. The diamond structure is well known as occurring in carbon and also in silicon and germanium, while the *Imma* structure occurs in silicon and germanium [24]. We calculated the $P4_132$ sixfold coordinated structure proposed by Ma *et al.* [9] to be roughly 100 meV per atom higher in enthalpy than our $P4_2/mbc$ structure over the range 200–600 GPa, and it is never the most stable structure. The reason for this discrepancy is not entirely clear to us although, as noted above, the results are sensitive to the pseudopotential core radius, and we have obtained similar results to Ma *et al.* when using radii which are too large. We therefore conclude that the coordination number of Li atoms increases from three to four at high pressures, in agreement with Tamblyn *et al.* [10] Our estimate of the transition pressure of 449 GPa is likely to be an overestimate because we have neglected quantum zero point motion which favors more closely packed structures. It is expected that all elements will form close-packed structures under sufficient compression, but this must occur at extremely high pressures in Li.

The e-DOS of the higher-pressure $P4_2/mbc$ and diamond-structure phases are shown in Fig. 3(b) at 450 GPa, which is close to their coexistence pressure, along with the e-DOS of the fcc phase. At this pressure the occupied valence bandwidths are 19% (fcc), 24% ($P4_2/mbc$), and 38% (diamond) of their respective free-electron values. The e-DOS of fcc has a strong peak just below E_F and the e-DOS at E_F is 44% of the free-electron

value. The e-DOS of the diamond structure and $P4_2/mbc$ phases show pronounced dips around E_F . The e-DOS of the diamond structure at E_F is 29% of the free-electron value, while that of $P4_2/mbc$ is only 6% of the free-electron value. The mechanisms of band narrowing in the lower portion of the valence band and the increased stability of phases such as $P4_2/mbc$ and the diamond structure associated with a reduction in the e-DOS near E_F still operate at very high pressures.

The bands arising from the $1s$ core electrons are ~ 45 eV below E_F at 75 GPa and ~ 50 eV below at 450 GPa. The structures with short nearest-neighbor distances tend to have wider core bandwidths, and the core bandwidths increase with pressure. At 75 GPa, the core bandwidths are substantially smaller than the occupied valence bandwidths although in $Cmca-24$, which has the shortest nearest-neighbor separation of the structures appearing in Fig. 3(a), the core bandwidth is 50% of the occupied valence bandwidth. At 450 GPa the core bandwidths are considerably larger, and for the structures appearing in Fig. 3(b) the core bandwidth is roughly twice the occupied valence bandwidth.

Lithium develops a novel electronic structure under high pressures. The valence electrons are pushed away from the ionic cores and form piles of charge at interstitial locations. These piles of electronic charge are rather isolated from one another, and the occupied valence bandwidths of the high-pressure phases are narrower than the corresponding free-electron values, in accord with the picture developed by Rousseau and Ashcroft [5]. The situation is strongly reminiscent of an “electride” [25], in which the electrons play the role of the anions. At high pressures we predict the most stable structure to consist of Li ions arranged in the diamond structure. In this structure the Li ions and the valence electron sites form interpenetrating diamond lattices and, taking the Li and electron sites together, they form the B32 (NaTl-type) Zintl structure. This structure is adopted by several ionic AB compounds with A^+ ions from group I of the periodic table (Li, Na, and K) and B^- ions from group III (Al, Ga, In, and Tl) [26].

In conclusion, we find that the most stable phases of Li have threefold coordination in the pressure range 40–450 GPa, but fourfold coordination from 450 GPa up to pressures beyond 1 TPa. The return to close-packed structures must occur at extremely high pressures beyond the reach of current static diamond-anvil-cell experiments. We found new distortions of the $Cmca-24$ structure, including one of $Pbca$ symmetry which is energetically favorable at lower pressures. Our prediction of several nearly degenerate phases in the pressure range 86–110 GPa suggests the formation of disordered structures which, when combined with the very low e-DOS at E_F might result in semiconducting behavior. We predict that the $Cmca-24$ structure becomes unstable to a $P4_2/mbc$ phase at 247 GPa, and that

at still higher pressures a diamond structure is formed. We have suggested that the high-pressure phases of Li can be described as elemental electrides.

The authors were supported by the Engineering and Physical Sciences Research Council (EPSRC) of the UK.

-
- [1] C. S. Barrett, *Acta Crystallogr.* **9**, 671 (1956).
 - [2] J. B. Neaton and N. W. Ashcroft, *Nature (London)* **400**, 141 (1999).
 - [3] M. Hanfland, K. Syassen, N. E. Christensen, and D. L. Novikov, *Nature (London)* **408**, 174 (2000).
 - [4] We refer to the symmetries of structures by their short Hermann-Mauguin space group symbols.
 - [5] B. Rousseau and N. W. Ashcroft, *Phys. Rev. Lett.* **101**, 046407 (2008).
 - [6] V. V. Struzhkin, M. I. Eremets, W. Gan, H.-k. Mao, and R. J. Hemley, *Science* **298**, 1213 (2002).
 - [7] A. F. Goncharov, V. V. Struzhkin, H.-k. Mao, and R. J. Hemley, *Phys. Rev. B* **71**, 184114 (2005).
 - [8] R. Rousseau, K. Uehara, D. D. Klug, and J. S. Tse, *Chem. Phys. Chem.* **6**, 1703 (2005).
 - [9] Y. Ma, A. R. Oganov, and Y. Xie, *Phys. Rev. B* **78**, 014102 (2008).
 - [10] I. Tamblyn, J.-Y. Raty, and S. A. Bonev, *Phys. Rev. Lett.* **101**, 075703 (2008).
 - [11] K. Shimizu, H. Ishikawa, D. Takao, T. Yagi, and K. Amaya, *Nature (London)* **419**, 597 (2002).
 - [12] K. Shimizu, D. Takao, S. Furomoto, and K. Amaya, *Physica (Amsterdam)* **408C**, 750 (2004).
 - [13] V. E. Fortov, V. V. Yakushev, K. L. Kagan, I. V. Lomonosov, V. I. Postnov, T. I. Yakusheva, and A. N. Kuryanchik, *JETP Lett.* **74**, 418 (2001).
 - [14] M. Bastea and S. Bastea, *Phys. Rev. B* **65**, 193104 (2002).
 - [15] C. J. Pickard and R. J. Needs, *Phys. Rev. Lett.* **97**, 045504 (2006).
 - [16] C. J. Pickard and R. J. Needs, *Nature Phys.* **3**, 473 (2007).
 - [17] C. J. Pickard and R. J. Needs, *Phys. Rev. B* **76**, 144114 (2007).
 - [18] C. J. Pickard and R. J. Needs, *Nature Mater.* **7**, 775 (2008).
 - [19] S. J. Clark, M. D. Segall, C. J. Pickard, P. J. Hasnip, M. I. J. Probert, K. Refson, and M. C. Payne, *Z. Kristallogr.* **220**, 567 (2005).
 - [20] D. Vanderbilt, *Phys. Rev. B* **41**, 7892 (1990).
 - [21] J. P. Perdew, K. Burke, and M. Ernzerhof, *Phys. Rev. Lett.* **77**, 3865 (1996).
 - [22] See EPAPS Document No. E-PRLTAO-102-074916 for details of new structures, phonons of $P4_2/mbc$, and e-DOS of $Cmca-24$, $Pbca$, and $Aba2$ phases. For more information on EPAPS, see <http://www.aip.org/pubservs/epaps.html>.
 - [23] J. S. Tse, D. D. Klug, and T. Iitaka, *Phys. Rev. B* **73**, 212301 (2006).
 - [24] A. Mujica, A. Rubio, A. Muñoz, and R. J. Needs, *Rev. Mod. Phys.* **75**, 863 (2003).
 - [25] J. L. Dye, *Science* **301**, 607 (2003).
 - [26] J. Evers and G. Oehlinger, *Inorg. Chem.* **39**, 628 (2000).